MICROBIOLOGY

Cultivation of Methanonezhaarchaeia, the third class of methanogens within the phylum Thermoproteota

Anthony J. Kohtz[1]*†, Sylvia Nupp[1], Roland Hatzenpichler[1,2]*

Methane is a potent greenhouse gas, largely produced by methanogenic archaea, contributing to Earth's dynamic climate and biogeochemical cycles. In the past decade, metagenomics revealed that lineages outside of the Euryarchaeota superphylum encode genes for methanogenesis. This was recently confirmed through the cultivation of two classes of methanogenic Thermoproteota. Thus far, all methanogens within the Thermoproteota are predicted or were shown to be methylotrophic. The only exception to this are the Nezhaarchaea, for which metagenomic predictions suggest they are CO_2-reducing methanogens. Here, we demonstrate methanogenic activity in a third class of Thermoproteota, the Methanonezhaarchaeia. Contrary to genomic predictions for this class, we cultivated a methylotrophic species, *Candidatus* Methanonezhaarchaeum fastidiosum YNP3N, highlighting the importance of testing metagenomic hypotheses through experimentation. We investigate the metabolic diversity of Methanonezhaarchaeia, including metabolic modifications accompanying frequent loss of methanogenesis in this class. This highlights gaps in our understanding of the biochemistry, diversity, and evolution of thermoproteotal methanogens and their contributions to carbon cycling.

INTRODUCTION

Methanogenesis, the production of methane coupled to energy conservation, is a uniquely archaeal metabolism (*1*, *2*). Phylogenetic reconstructions and geological evidence indicate that methanogenesis was among the earliest metabolisms to evolve and that the last archaeal common ancestor likely was a methanogen (*3*–*7*). Through their activity, methanogens are responsible for mediating global methane emissions, which substantially affect Earth's climate (*8*). While all methanogens share a unique methane-forming enzyme, methyl coenzyme M reductase (MCR), different precursor molecules can be converted to methane via distinct pathways: (i) CO_2-reducing, (ii) acetoclastic, (iii) methyl-dismutating, (iv) methyl-reducing, (v) methoxyl-dismutating, and (vi) alkylotrophic methanogenesis (*1*).

In addition to discoveries regarding their metabolism (*9*–*12*), our understanding of which archaea engage in methanogenesis has radically changed over the past decade. Traditionally, all methanogens were thought to belong to the superphylum Euryarchaeota. However, this view rapidly changed after several independent metagenomic studies discovered genes for anaerobic alkane-cycling in numerous uncultured archaeal lineages within the phylum Thermoproteota (also known as TACK superphylum), including Korarchaeia (*10*, *12*), Methanomethylicia (previously called Verstraetearchaeota) (*13*), Nezhaarchaea (*14*), Nitrososphaeria (*15*, *16*), Aukarchaeles (*17*), and Bathyarchaeia (*18*, *19*). In addition, even within Euryarchaeota, multiple deep branching methanogenic and alkane degrading lineages have been discovered in the past decade, showing our understanding of the mediators of these metabolisms are not yet complete (*10*, *11*, *14*, *20*–*23*). Only recently, the first three cultures of Korarchaeia (one enrichment) and Methanomethylicia (one enrichment and one isolate) were recovered, enabling an experimental validation of their methanogenic physiology (*17*, *24*, *25*). The expansion in experimentally confirmed as well as potential thermoproteotal methanogens has wide-ranging implications for our understanding of global methane cycling, the evolution and biology of archaea, and the biotechnological potential of these previously unknown methanogens (*1*, *3*, *4*, *16*, *26*).

Almost all lineages of (potential) methanogens within the Thermoproteota are predicted (*10*, *12*–*19*) or have been demonstrated (*17*, *24*, *25*) to live by methyl-reducing methanogenesis. Methylated methanogenic precursors are widely distributed in anoxic habitats and methyl-reducing methanogenesis is the dominant form of methanogenesis in anoxic marine, freshwater, and hypersaline sediments according to isotope tracer studies (*27*). The methyl-reducing nature of many thermoproteotal methanogens is supported by the presence of methyltransferase genes and the lack of both the Wood-Ljungdahl pathway (WLP) and the tetrahydromethanopterin *S*-methyltransferase (MTR) that can connect methanogenesis to the WLP. So far, the only lineage within the Thermoproteota that encodes both MCR and MTR are the "Nezhaarchaea," which, based on metagenomics, are predicted to be CO_2-reducing methanogens (*14*, *16*). Nezhaarchaea were first discovered in hot spring samples (*14*, *16*) but are also present in deep-sea hydrothermal systems (*28*), suggesting that they are important for methane cycling in high temperature environments. So far, the only experimental evidence supportive of a methanogenic lifestyle was a study demonstrating that Nezhaarchaea are the most abundant MCR-encoding archaea in some hot springs and transcribe MCR in methanogenic microcosms seeded with biomass from those hot springs (*29*). While this was an important step forward, most of their metabolism remains unresolved due to low recruitment of metatranscriptomic reads to genes beyond MCR and Nezhaarchaea remain enigmatic without cultures.

Here, we demonstrate methylotrophic methanogenesis in the Nezhaarchaea through selective cultivation, fluorescence microscopy, and metagenomic and metatranscriptomic sequencing. We further assess the wider metabolic diversity across this lineage, for which we propose the updated name Methanonezhaarchaeia, suggesting

[1]Department of Chemistry and Biochemistry, Center for Biofilm Engineering, and Thermal Biology Institute, Montana State University, Bozeman, MT 59717, USA. [2]Department of Microbiology and Cell Biology, Montana State University, Bozeman, MT 59717, USA.
*Corresponding author. Email: anthony.kohtz@monash.edu (A.J.K.); rolandhatzenpichler@gmail.com (R.H.)
†Present address: Department of Microbiology, Biomedicine Discovery Institute, Monash University, Clayton, VIC 3800, Australia.

that the loss of methanogenesis across this lineage is associated with rewiring of membrane-associated redox complexes.

RESULTS AND DISCUSSION

Cultivation of a previously unknown methylotrophic methanogen

We recently demonstrated the Lower Culex Basin (LCB) in Yellowstone National Park to be an area hosting a taxonomically diverse range of previously unknown MCR-encoding archaea affiliated with the superphylum Thermoproteota (*30*). Notably, methanogenic cultures of the first two classes of thermoproteotal methanogens, affiliating to the Korarchaeia and Methanomethylicia, were obtained from hot springs located in the LCB (*24*, *25*). Furthermore, mesocosm experiments using sediments from hot spring "LCB003" revealed that members of a third class of thermoproteotal MCR-encoding archaea, Nezhaarchaea, became slightly enriched (up to 8% relative abundance) under methanogenic conditions when incubated with methanol under a N_2/CO_2 headspace (*30*). We also observed that hot spring LCB003 exhibited a large methane flux of 5.9 ± 4.6 mmol CH_4 m^{-2} day^{-1} ($n = 3$ replicates).

To further explore the metabolism of Nezhaarchaea and attempt their cultivation, we incubated sediments from hot spring LCB003 in anoxic media under a variety of conditions designed to stimulate methylotrophic methanogenesis at the in situ temperature of 77°C and pH of 6.5. We found that incubations with monomethylamine (MMA), dimethylamine, or trimethylamine, with or without isopropanol, and a N_2/CO_2 headspace repeatedly led to the enrichment of Nezhaarchaea along with pronounced methane production (Fig. 1 and fig. S1). Further incubations revealed that isopropanol is not required for enrichment and has little effect on total methane production (Fig. 1A). MMA exhibited the most consistent response in methane production, and all further work was performed using MMA as a substrate. The cultures exhibited long lag times of around 50 to 60 days when first inoculated into anoxic media, and this response was repeatable over multiple years of sampling from the same hot spring. Cultures were found to be slow growing and fastidious, and they frequently stopped growing after one to two transfers into fresh media; however, we were able to eventually obtain a stable methanogenic culture for detailed study (Fig. 1).

We found that incubations initiated with 50% H_2 in the headspace did not develop any significant enrichment of Nezhaarchaea, suggesting that they may be adapted to low H_2 concentrations or are outcompeted under those conditions. In contrast, the methanogenic korarchaeon *Ca.* Methanodesulfokora washburnensis, which we previously enriched from the same hot spring, rapidly increases in abundance under a 50% H_2 headspace and methanol amendment (*24*). This indicates that these thermoproteotal methanogens inhabit different niches within the same hot spring sediment with regard to both substrate (methylamines versus methanol) and hydrogen (no/low H_2 versus high H_2) preferences.

Long-read Nanopore and short-read Illumina sequencing of the culture recovered a complete circular genome of the nezhaarchaeon, with a size of 1.75 Mbp and a GC content of 53% (table S1). Read mapping of the short read metagenome to the genome revealed that this archaeon dominated the culture at a relative abundance of 90.13% (Fig. 1B and table S1). This enrichment is consistent with qualitative assessments of Methanonezhaarchaeia populations by fluorescence in situ hybridization (FISH) that also revealed a high enrichment of Methanonezhaarchaeia (Fig. 1C), and >98% of reads from metatranscriptomic analysis mapping to strain YNP3N. In contrast, by mapping the raw reads of the LCB003 hot spring metagenome to the genome of the archaeon in culture, we estimate the relative abundance of the organism in its native habitat to be 0.46%. Phylogenomic, average nucleotide identity (ANI), and GTDB-tk analyses showed that the cultured archaeon clusters within the Nezhaarchaea lineage and that it represents a previously unknown species, for which we propose the name *Candidatus* Methanonezhaarchaeum fastidiosum strain YNP3N (Fig. 2A, fig. S2, and table S1). We chose this name to emphasize the "methano-" prefix typical in methanogen taxonomy, to preserve previously proposed names as much as possible [i.e., Nezhaarchaeota and Nezhaarchaea (*14*, *16*, *29*)], and to emphasize the fastidious and slow-growing nature of this organism. We note that this name change will necessitate slightly renaming this group using the type genus *Methanonezhaarchaeum* propagated up to class Methanonezhaarchaeia (see the "Etymology" section at the end of the manuscript and the "Protolog" section in the Supplementary Materials).

Strain YNP3N encoded the only *mcrA* gene recovered in the metagenome assembly, and phylogenetic analysis of this gene placed it within the Methanonezhaarchaeia, with recently described Bathyarchaeia sequences as a sister group (Fig. 2B) (*18*). We also found fragmented *mcrBCD* genes related to *Ca.* Methanoglobus hypatiae (*21*), known to metabolize MMA, in the metagenome assembly. However, no

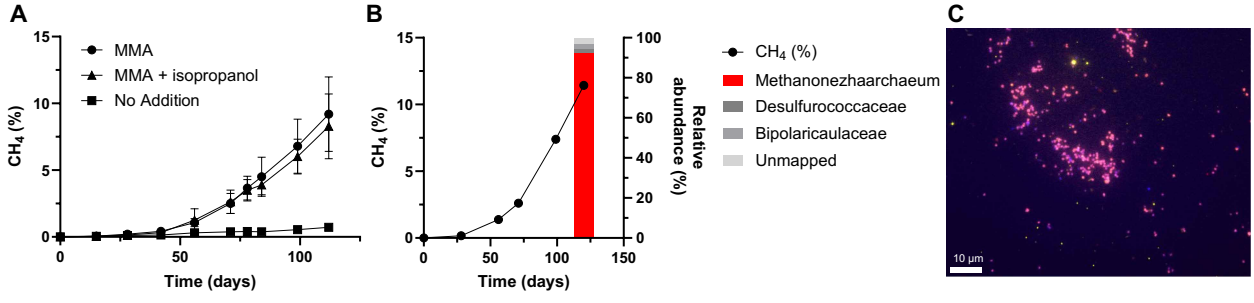

Fig. 1. Enrichment cultivation and visualization of *Ca.* Methanonezhaarchaeum fastidiosum YNP3N. (**A**) Methane production by the culture under varying amendments: MMA only ($n = 9$), MMA and isopropanol ($n = 9$), and no addition ($n = 3$). Symbols are the mean from biological replicates and error bars are one SD. Where not visible the error bars are smaller than the symbol. (**B**) Long-term cultivation on MMA and multiple transfers produced a sediment-free culture >90% enriched in strain YNP3N according to metagenomics ($n = 1$). (**C**) Fluorescence microscopy image of Methanonezhaarchaeia cells imaged by FISH. Abundant coccoid cells double hybridized (appearing in pink) with a general archaeal probe (Arch915, red) and a probe specific to Methanonezhaarchaeia (Mnez277, yellow). Cells were counterstained with DAPI (blue). Bright yellow signals stem from autofluorescent sediment particles.

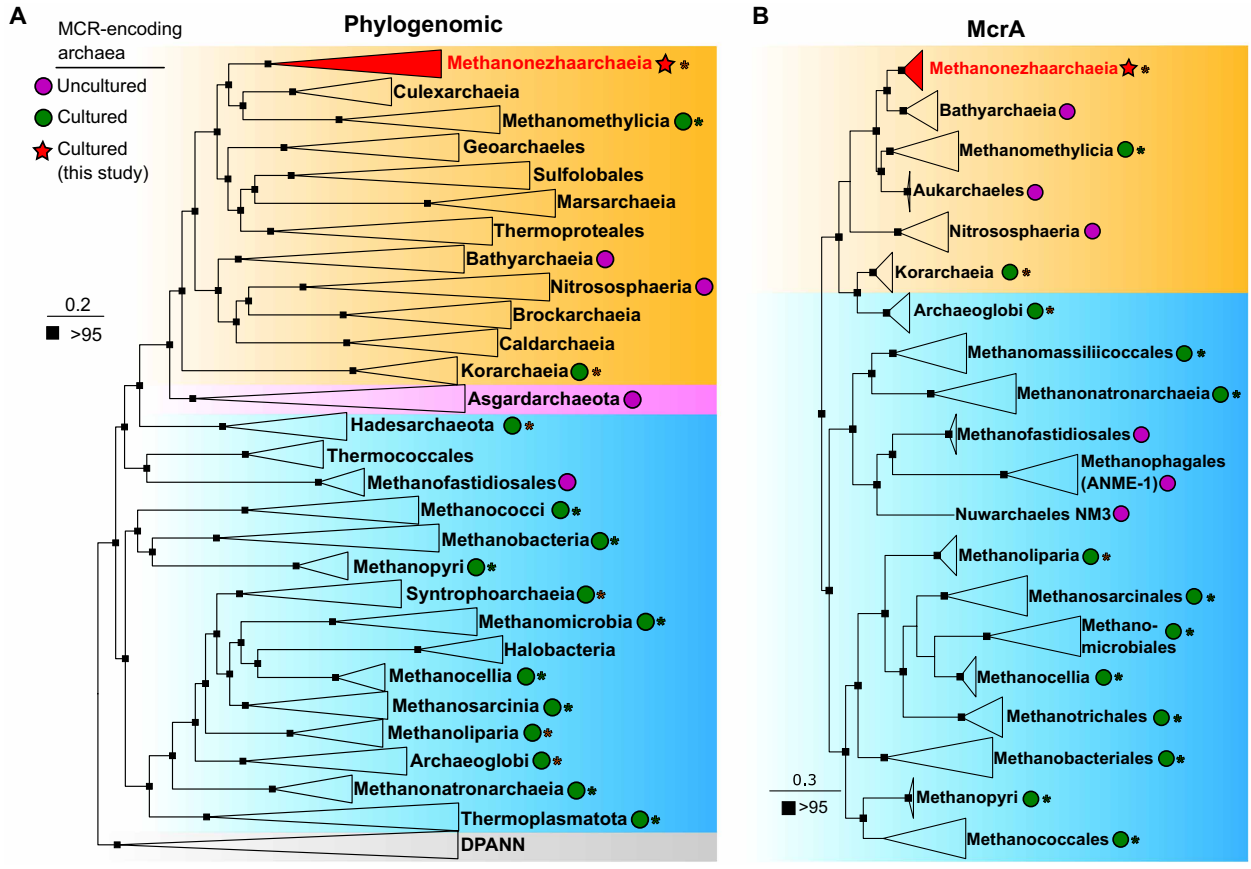

Fig. 2. Phylogenetic placement of Methanonezhaarchaeia based on single copy marker genes and McrA. (**A**) Phylogenomic tree of archaea based on a set of 43 single-copy marker genes. Major groups of archaea are highlighted in orange (Thermoproteota/TACK superphylum), pink (Asgardarchaeota), blue (Euryarchaeota), and gray (DPANN). For inclusion, genomes were required to have at least 37 of the marker genes. Squares at the nodes indicate ultrafast bootstrap support, only values above 95 are shown. (**B**) Phylogenetic tree of McrA sequences demonstrating the affiliation of YNP3N within the Methanonezhaarchaeia (Thermoproteota, orange) compared to Euryarchaeota (blue). Squares at the nodes indicate ultrafast bootstrap support, only values above 95 are shown. Asterisks by cultured lineages indicate where isolates (green) or enrichments (orange) have been obtained.

Methanoglobus *mcrAG* was recovered, the *mcrBCD* genes had low coverage, and mapping the metagenomic reads to the *Ca.* M. hypatiae genome revealed a relative abundance of 0.037%. Together, this suggests minimal impacts on the observed methane production by *Ca.* M. hypatiae. We also observed a second species of Methanonezhaarchaeia in the culture, with a low relative abundance of 1.86%. However, the MAG was noncircular, less complete (85.29%), and did not encode *mcr* genes (table S1).

A FISH probe was designed to target Methanonezhaarchaeia. Application of this probe and a general archaeal probe revealed abundant coccoid cells that were labeled with both probes, confirming the high enrichment of Methanonezhaarchaeia (Fig. 1C). Searches against public databases using the 16*S* rRNA and *mcrA* gene sequences as queries showed that Methanonezhaarchaeia are found globally in terrestrial hot springs and marine hydrothermal systems (tables S2 and S3). However, it is important to note that Methanonezhaarchaeia were likely overlooked in the past because commonly used polymerase chain reaction primers exhibit multiple mismatches to their *mcrA* genes (*30*).

Metabolism and gene expression

Reconstruction of the metabolic potential revealed that strain YNP3N encodes a more diverse metabolism for methanogenic substrates relative to previously published Methanonezhaarchaeia MAGs, which had been proposed to exclusively use H_2/CO_2 for methanogenesis. As expected, the MCR complex genes were highly expressed during methanogenic growth. During growth on MMA, YNP3N highly expresses methyltransferase genes involved in the metabolism of this substrate (*mtmB* and *mtbC*) and expresses genes for using other methylamines (*mtbB* and *mttB*) at a lower level (Fig. 3B). While there was not an associated *mtbA* gene, an *mtaA*-like gene is colocated and highly expressed, likely replacing the activity of *mtbA*, similar to the methyltransferase systems found in Methanomassillicoccales (*31*) and *Ca.* Methanglobus hypatiae (*21*). We also identified pyrrolysine biosynthesis genes, PylSBCD, and a Pyl-tRNA used to recode stop codons, notably found within the methylamine methyltransferase genes (*32*–*34*). Furthermore, we observed expression of diverse corrinoid transporter genes and cobalamin-binding proteins required for import of vitamin B_{12} and synthesis of cobalamin proteins found in methyltransferase systems (*35*, *36*). This indicates the importance of this vitamin in the metabolism of this organism and suggests that in the native hot spring, these transporters are likely important in uptake of B_{12} from the environment. Strain YNP3N also expressed both the tetrahydromethanopterin MTR complex and the methyl branch of the WLP, further indicating its capability for methyl-dismutating methanogenesis.

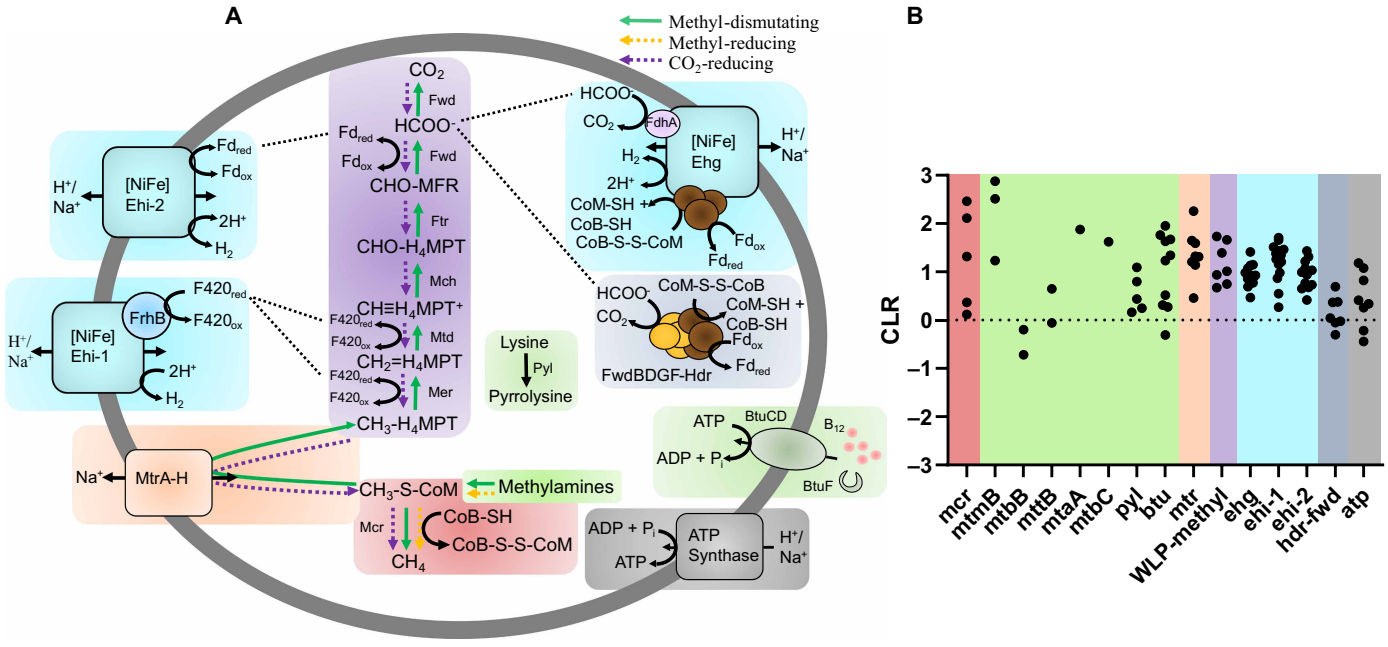

Fig. 3. Proposed methane, hydrogen, and formate metabolism in Ca. *M. fastidiosum* YNP3N. (**A**) Metabolic reconstruction of methanogenesis, energy conservation, and vitamin B12 import in YNP3N. A list of genes used to construct this figure can be found in table S4. (**B**) Gene expression of YNP3N during growth on MMA ($n = 1$ due to low RNA yields) suggests a methyl-dismutating methanogenic lifestyle. Dotted line represents the geometric mean expression of all genes. Unless a specific subunit is listed, each dot represents the expression of a subunit in a multisubunit enzyme or functional class, or expression of multiple copies of a particular gene. Explicit values can be found in table S5.

This is in stark contrast to previously cultured Thermoproteota methanogens, which all lack a full MTR complex and most lack the WLP (*1*, *15*, *17*, *24*, *25*). We could not sustain growth of strain YNP3N without addition of MMA as a growth substrate, even with CO_2/bicarbonate present, suggesting that YNP3N, contrary to its genomic potential, does not perform CO_2-reducing methanogenesis in vitro. These findings highlight the importance of testing predictions from (meta)genomics through careful experiments and the indispensability of cultivation.

When the culture was incubated with ^{13}C-labeled MMA, we found that both ^{13}C-CH_4 and ^{13}C-CO_2 were produced, further evidencing that methyl-dismutating methanogenesis is occurring (Fig. 3 and fig. S3A). During the isotope tracer experiment, we also measured low concentrations of H_2 (up to 35 μM above background; fig. S3B), similar to what is observed for methylotrophic and hydrogenotrophic *Methanosarcina* species in which the oxidation of one methyl group provides enough reducing equivalents, with H_2 as an intermediate, to fuel the reduction of three methyl groups to methane (*37*). In our experiment, we observed CH_4:CO_2 ratios of ~1:1, which may reflect differences in the energy conservation pathways of strain YNP3N compared to previously characterized methyl-dismutating methanogens. In cytochrome-containing methylotrophic *Methanosarcinales*, a membrane bound HdrDE is either used in a H_2-dependent fashion with [NiFe] hydrogenases, or in an H_2-independent fashion with Fpo or Rnf (*1*, *2*, *37*). These membrane-bound electron transport chains are more efficient than those found in methanogens without cytochromes (*1*, *2*, *37*). Since, to our knowledge, strain YNP3N represents the first cultured methyl-dismutating methanogen without cytochromes (HdrDE), the commonly cited 3:1 ratio of CH_4:CO_2 observed in *Methanosarcinales* may not be universal among methyl-dismutating methanogens (*1*, *2*, *37*). Other factors impacting the observed ratio could also include (i) leaky H_2-cycling, i.e., H_2 not being captured efficiently, or other coenriched microbes contributing to H_2-uptake, or (ii) carbon from methylamine being diverted into biosynthetic pathways through the WLP (*38*–*41*).

For heterodisulfide reduction, methanogens lacking cytochromes commonly have an electron-bifurcating cytoplasmic Mvh-Hdr complex that allows coupling the oxidation of H_2 to the reduction of ferredoxin and heterodisulfide (*42*). In formate-using methanogens, Mvh-Hdr can also form large complexes with FdhAB, to allow formate to substitute for H_2 as an electron donor (*43*). YNP3N lacks FdhAB or MvhABG associated with a soluble HdrABC operon. Instead, a second gene cluster containing FwdBD subunits are found colocated with HdrABC in the YNP3N genome. The FwdBD subunits typically perform CO_2 reduction to formate in hydrogenotrophic methanogens, with formate then migrating to the FwdA subunit (*44*, *45*). Thus, this Fwd-Hdr complex may enable formate oxidation to be coupled with heterodisulfide and ferredoxin reduction. The additional colocated FwdF polyferredoxin and FwdG genes would likely allow to electronically couple the HdrABC and FwdBD subunits. This Fwd-Hdr organization is a strategy distinct from the characterized Fmd-Hdr-Fdh or Fwd-Hdr-Mvh-Fdh complexes found in *Methanosprillium* or *Methanococcus*, respectively (*43*, *46*). Strain YNP3N also expresses a separate FwdABCD gene cluster colocated with other genes of the WLP, and here, the FwdBD genes are fused, indicating gene duplication and fusion events enabled a repurposing of the second Fwd complex for involvement in heterodisulfide cycling.

Furthermore, for formate, hydrogen, and heterodisulfide cycling, YNP3N also expressed a membrane associated group 4 [NiFe]-hydrogenase colocated with HdrABC and formate dehydrogenase

(FdhA) subunits, termed Ehg (Fig. 3 and fig. S4) (*47*). Thus, this complex may be able to couple the oxidation of H_2 or formate to the reduction of heterodisulfide and ion translocation for energy conservation. The FdhA subunit in YNP3N is similar in sequence (35 to 38% sequence identity) to those found in formate oxidizing methanogens within the Methanococcales, Methanobacteriales, and Methanocellales (*48*–*50*). However, with the presence of HdrA, this complex may also be capable of flavin-based electron bifurcation and ferredoxin reduction. Unlike methanogens that use exogenous formate as an electron donor, no formate transporters were found in the YNP3N genome, suggesting instead that internal formate cycling may occur, with formate being produced during methyl-oxidation through the WLP and then directly coupled to heterodisulfide reduction at the Fwd-Hdr or Ehg complexes (Fig. 3) (*48*–*50*). Consistent with the predicted absence of a formate transporter, attempts to grow strain YNP3N with MMA on a range of exogenous formate concentrations (2, 10, and 100 mM) were unsuccessful (not shown).

In addition, YNP3N encodes several other [NiFe] hydrogenases, suggesting that internal hydrogen cycling mechanisms could fuel methyl-dismutating methanogenesis. One expressed membrane bound group 4 [NiFe]-hydrogenase complex (Ehi-1, Fig. 3 and fig. S4) is flanked by *frhB*, suggesting that this complex is involved in the oxidation of reduced F_{420} that could be produced by oxidizing methyl groups via the WLP during methyl-dismutating methanogenesis. Strain YNP3N encodes the biosynthetic pathway for producing F_{420}, and we could not identify any other genes outside of *frhB* involved in recycling the F_{420} cofactor. A second expressed membrane bound group 4 [NiFe]-hydrogenase may deal with ferredoxin recycling produced by Fwd during methyl oxidation. This reduced ferredoxin could be oxidized by a second group 4 [NiFe] hydrogenase (Ehi-2, Fig. 3 and fig. S4) coupled with transport of ions across the membrane and the production of H_2. Recycling of hydrogen produced through methyl oxidation may be recaptured by the Ehg hydrogenase complex, allowing for the direct coupling of heterodisulfide reduction and energy conservation.

Our analysis of strain YNP3N suggests that the use of multiple substrate and electron donor pools (methyl groups, H_2, formate) may enable resilience during changing environmental conditions, as found in dynamic geothermal systems. Consistent with this, Methanonezhaarchaea have been observed to be stable populations and are often the dominant MCR-encoding organism in several hot spring systems (*29*, *30*).

Evolution and diversity of Methanonezhaarchaeia

The discovery of methylotrophic methanogenesis in the Methanonezhaarchaea, which previously had been predicted to only perform CO_2-reducing methanogenesis, led us to reassess the wider metabolic diversity of this lineage. We observed 13 different species clusters, comprising three families within the Methanonezhaarchaeales, which we propose as "Methanonezhaarchaeceae" (f__WYZ-LMO8), "Muzhaarchaeceae" (f__B40-G2), and "Jinzhaarchaeceae" (f__JAWCJE01) (Fig. 4A and table S5).

Ca. M. fastidiosum YNP3N was the only genome found to contain genes for biosynthesis of pyrrolysine and methyltransferases for

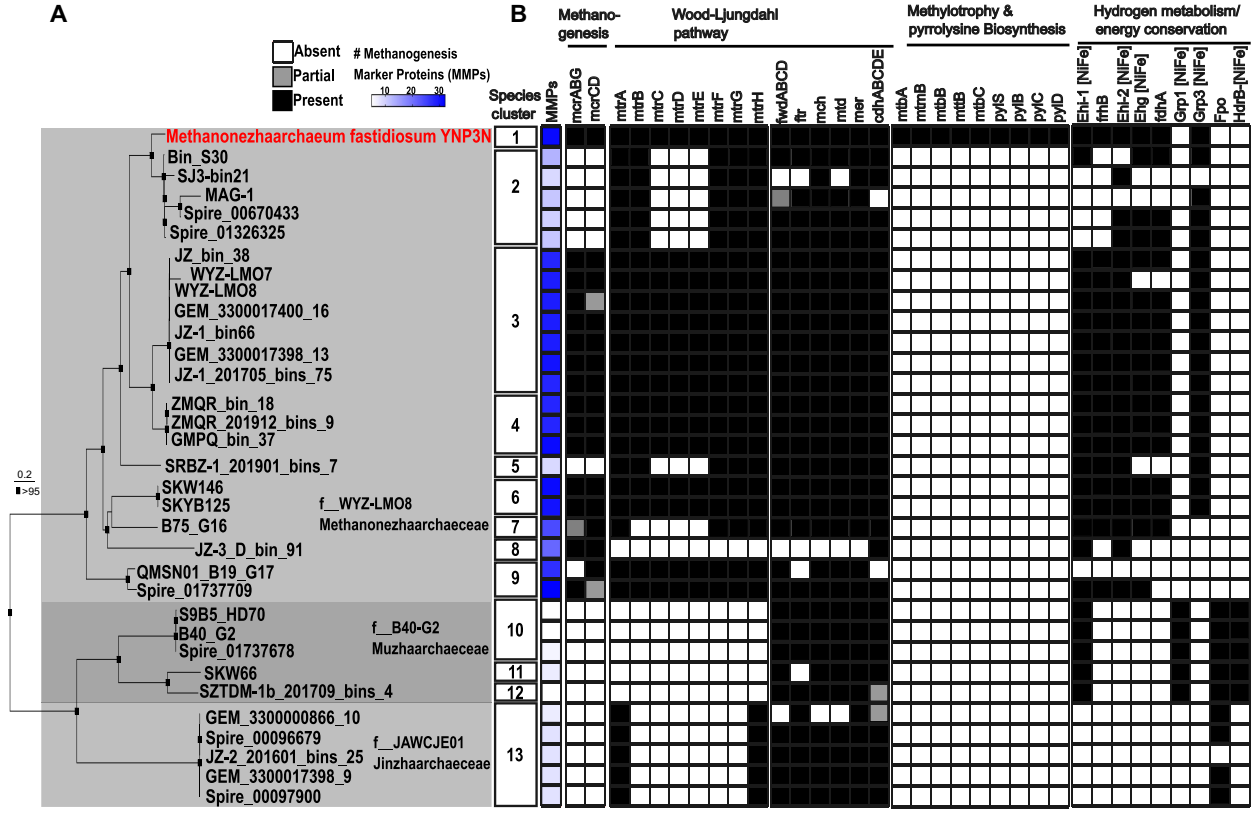

Fig. 4. Comparative genomics of three families within Methanonezhaarchaeia. (**A**) Genome tree illustrating the diversity of Methanonezhaarchaeia. The phylogenetic tree shown here is a subset of the tree shown in Fig. 2A. (**B**) Presence and absence of key metabolic genes and methanogenesis marker proteins.

methylamines, indicating its unique capability for methylotrophic methanogenesis. We found that while nearly all Methanonezhaarchaeia species encode a complete or partial *mcrABGCD*, all MAGs affiliated with its sister groups, Muzhaarchaeceae and Jinzhaarchaeceae, lacked these genes. This suggests a transition from a methanogenic to nonmethanogenic lifestyle within the class Methanonezhaarchaeia. Consistent with this, all members of the Muzhaarchaeceae and Jinzhaarchaeceae, in addition to two species clusters within the Methanonezhaarchaeceae, encoded only a limited subset of the 38 methanogenesis marker proteins, including the one most closely related to strain YNP3N (87.4% ANI) (Fig. 4B and table S6).

Furthermore, different patterns of MTR presence-absence were observed, with Muzhaarchaeceae seemingly having lost this complex together, while members of the Jinzhaarchaeceae only encode the MtrA and MtrH subunits. Five of nine species clusters within the Methanonezhaarchaeceae encode a full MTR complex, while one lacked it completely, and three species clusters were missing MtrCDE. MtrCDE subunits interact in sodium ion pumping, and their loss could indicate an important intermediate stage in the loss of methanogenic potential, by uncoupling MTR from energy conservation in species that have already lost MCR (Fig. 4) (*51*). Furthermore, the *mtrA* gene found in Jinzhaarchaeceae has a separate evolutionary history from those found in Methanonezhaarchaeceae, as it branches with sequences from the Asgardarchaeota while Methanonezhaarchaeceae sequences branch with Bathyarchaeia (fig. S5). Together, this is further evidence for a complicated history of loss and horizontal gene transfer of the MTR subunits in addition to repurposing of at least the MtrAH subunits in diverse nonmethanogenic lineages (*3*, *4*, *52*).

Compared to the pattern observed for MTR, the methyl and carbonyl branches of the WLP were largely conserved across all three families. This is consistent with the highly flexible nature of this pathway that is connected to methanogenesis through MTR, but also serves multiple separate catabolic and anabolic roles in methanogenic and nonmethanogenic microbes, including the biosynthesis of purines, thymidylate, methione, and acetyl–coenzyme A (*39*–*41*).

For Methanonezhaarchaeceae, the membrane associated energy conservation and redox modules are largely conserved across the nine identified species clusters, with numerous group 4 [NiFe] hydrogenases, including the HdrB- and FdhA-associated Ehg complex and the FrhB-associated Ehi-2 complex (Figs. 3 and 4). For Muzhaarchaeceae, we observed a large remodeling of membrane associated complexes, with a group 1 [NiFe] hydrogenase, Fpo, and a group 4 HdrB-associated [NiFe] hydrogenase similar to the Ehd complex found in the Methanomethylicia and Culexarchaeia (Fig. 4 and fig. S4) (*10*, *47*). In contrast, Jinzhaarchaeceae exhibit a more minimalistic electron transport chain, encoding a single Fpo-like complex. Further cultivation and high-quality genomes of diverse Methanonezhaarchaeia are required to further untangle the stepwise modifications of MTR, hydrogenases, and Fpo-like complexes that lead to a loss of methanogenic potential and the repurposing of the enzymatic remnants of methanogenesis into a new lifestyle.

Together, our results confirm methanogenesis in a third lineage of Thermoproteota, the Methanonezhaarchaeia. We expand the metabolic diversity of this group by cultivating a methylotrophic species from a group that hitherto had been assumed to only perform CO_2-reducing methanogenesis based on metagenomic predictions. These findings highlight the need for continued sampling of thermoproteotal methanogen genomes and cultures, which likely harbor further yet-unidentified diversity in their methanogenic pathways, and to test (meta)genomic prediction by experimentation. Multiple previously unknown gene arrangements of methanogenesis genes and associated redox and energy conserving complexes were identified in diverse Methanonezhaarchaeia genomes and found to be expressed in the YNP3N culture. This continues the trend of discoveries in methanogenic members of the Thermoproteota and identifies gaps in our understanding of the biochemistry and diversity of methanogens.

Methanogenesis was independently lost multiple times in archaea, leading to a patchy distribution of this metabolism (*3*, *4*, *10*). We further find that methanogenesis likely is not a feature of all members of the Methanonezhaarchaeia and suggest that this metabolic transition was driven by loss of methanogenesis genes (MCR and MTR) and remodeling of membrane associated energy conservation and redox modules. Obtaining more diverse cultures will aid in resolving the full metabolic diversity of these thermoproteotal methanogens and their close, yet uncultured, nonmethanogenic relatives.

Etymology

YNP3N is a methanogen affiliated with the phylum Thermoproteota (*14*) for which we propose the candidate status Methanonezhaarchaeum fastidiosum gen. nov. sp. nov. For a protolog, please see the Supplementary Materials.

Etymology: Me.tha.no.ne.zha.ar.chae'eum. N.L. pref. methano-, pertaining to methane metabolism; N.L. neut. pl. n. archaeum, "ancient", referring to the cell's affiliation to the archaeal domain; N.L. neut. n. Methanonezhaarchaeum, methanogen named after Nezha, an immortal in Chinese mythology (*14*). fas.ti.di.o'sum L. neut, adj. fastidiosum, referring to the fastidious growth of this organism. Locality: Sediment from a hot spring, identified as feature LCB003 (*30*). Diagnosis: A thermophilic methyl-dismutating methanogen of the phylum Thermoproteota that grows as coccoid cells.

METHODS

Source of inoculum and cultivation

Sediment was retrieved from hot spring LCB003 (44.57763, −110.78957; November 2022; 77°C; pH 6.5) as previously described and stored at room temperature (*24*, *30*). Methane flux from hot spring LCB003 was determined using a Li-COR 7810 trace gas analyzer on 27 July 2023. Three replicate measurements, each lasting 60 to 100 s were performed. Enrichment cultures were established using anoxic medium as previously described (*24*, *25*), with minor modifications. The medium had a pH of 6.5, containing a base of (per liter): KH_2PO_4, 0.5 g; $MgSO_4{\cdot}7H_2O$, 0.4 g; NaCl, 0.5 g; NH_4Cl, 0.4 g; $CaCl_2{\cdot}2H_2O$, 0.05 g; 2-*N*-morpholino-ethanesulfonic acid, 2.17 g; yeast extract, 0.1 g; and 0.002% (w/v) $(NH_4)_2Fe(SO_4)_2{\cdot}6H_2O$, 5 mM $NaHCO_3$, 1-ml trace element solution SL-10, 1-ml selenite-tungstate solution, 1-ml CCM vitamins (*25*), 0.0005% (w/v) resazurin, 10 mg of coenzyme M, 2-mg sodium dithionite, 1 mM dithiothreitol, and 1 mM $Na_2S{\cdot}9H_2O$. Sediment slurry was dispensed into serum bottles (10% v/v) and then sealed with thick butyl-rubber stoppers and aluminum crimps in an anoxic glove bag (Coy). The headspace of the enrichment was exchanged with N_2:CO_2 (90:10) gas for 5 min and set to 200 kPa. MMA was added to a final concentration of 10 mM. Cultures were incubated at 77°C upright in the dark and without shaking. While attempting to optimize our media and obtain a stable culture, we made the following modifications for the final media: (i) in the original incubation isopropanol was also added at a concentration of 10 mM, but was subsequently omitted from the medium, because it did not affect the

rate of growth or final methane concentration (ii) replaced $MgSO_4$ with $MgCl_2{\cdot}6H_2O$ at 0.33 g (per liter), and (iii) removed choline from the CCM vitamins. Transfers of these batch cultures were made with 20% (v/v) inoculum into fresh medium when methane concentrations reached 8 to 12%. Dimethylamine and trimethylamine were also tested for methane production with and without isopropanol. However, these higher amines led to more inconsistent methane production profiles relative to MMA, and we focused on MMA.

Gas chromatography and ^{13}C-MMA tracer incubations

Methane measurements were performed as described previously (*25*) using 250-µl headspace samples taken with a gas-tight syringe, injected into 10-ml vials sealed with gray chlorobutyl septa and aluminum crimps, and measured on a Shimadzu 2020-GC gas chromatograph.

For isotope tracer experiments, 60-ml serum vials with 30 ml of media and 30 ml of headspace were used. Enrichment cultures were inoculated (20% v/v) into medium with a final concentration of 10 mM ^{12}C-MMA. After 42 days, 2 mM ^{13}C-MMA was added to two replicates, and 2 mM ^{12}C-MMA was added to a control bottle. Headspace measurements were collected regularly as described to track the conversion of ^{13}C-MMA to ^{13}C-CH_4. Samples were analyzed using a Shimadzu QP2020 NX GCMS with a GS-CarbonPLOT column (30 m × 0.35 mm; 30 µm film thickness; Agilent). The instrument was operated in selected ion monitoring (SIM) mode as described previously (*25*). For quantification, peak areas corresponding to mass/charge ratios (m/z) of 16 for ^{12}C-CH_4, 17 for ^{13}C-CH_4, and 45 for ^{13}C-CO_2 were used. All injections on the Shimadzu 2020-GC were performed with a robotic autosampler (AOC-6000).

H_2 levels were tracked over the course of the isotope tracer experiment after bottles had been inoculated with ^{13}C-MMA. Samples were analyzed with an SRI Multi Gas 5 Gas Chromatograph with a thermal conductivity detector (oven temperature 50°C, thermal conductivity detector (TCD) temperature 100°C), using N_2 as a carrier gas.

DNA extraction and metagenome sequencing

Under anoxic conditions, 10 ml of the YNP3N culture were collected aseptically with a needle and syringe and concentrated on a sterile 0.2-µm polycarbonate membrane filter (Nuclepore) with vacuum filtration. The filter was then immediately placed into a Zymo BashingBead tube containing 750 µl of ZymoBIOMICS lysis solution. DNA was extracted using a ZymoBIOMICS DNA miniprep kit following the manufacturer's instructions. Illumina short-read library construction was performed with an Illumina DNA Prep kit following the manufacturer's instructions and was sequenced on an Illumina NovaSeq X Plus platform with 2 × 151-bp paired-end read chemistry performed at SeqCenter (Pittsburgh, PA, USA). Nanopore long-read sequencing was performed in-lab using a MinION platform and an R10.4.1 flow cell (Oxford Nanopore Technologies). Library preparation was performed using a rapid barcoding kit (SQK-RBK114.24) following the manufacturer's instructions and the flow cell was run for 27 hours. Base calling was performed with dorado (version 0.7.1) using model sup@v.5.0.0. The resulting BAM file was demultiplexed using dorado demux (--emit-fastq).

Metagenome assembly, polishing, binning, and quality assessment

An initial Nanopore assembly was performed with metaFlye (*53*) (version 2.9.4), which produced a circular assembly of the strain YNP3N genome. This genome was further polished using Illumina short reads using one round of Polypolish (version 0.6.0) followed by PyPolca (version 0.3.1; --careful) as recently suggested, given the high sequence coverage of the YNP3N genome (*54*, *55*).

A short-read assembly was also generated for analysis of coenriched microbes, with raw metagenomic reads with Illumina read quality, linker and adaptor trimming, artifact and common contaminant removal performed using the rqcfilter2 pipeline (maxns = 3 and maq = 20), and error correction with bbcms (mincount = 2 and hcf = 0.6) from the BBTools suite version 38.94 (Bushnell B. 2014. BBMap: a fast, accurate, splice-aware aligner; https://sourceforge.net/projects/bbmap). Resulting reads were then assembled with megahit (version 1.2.9; --k-list 27,37,47,57,67,77,87,97,107,117,127,141–mincount 1) (*56*). Coverage was determined by mapping reads to the assembly using minimap2 (version 2.26-r1175.; -x sr) (*57*). Contigs with a length of 2 kb or greater were used for binning with SemiBin2 (version 2.0.2). CheckM (version 1.1.3) was used to assess completeness and redundancy of the resulting MAGs (*58*). GTDB-tk (version 2.4.0) with the R220 release was used for assigning initial taxonomy (*59*). CoverM (version 0.7.0) with default settings was used to generate relative abundances of each MAG (*60*). CoverM was also used to estimate the relative abundance of the YNP3N genome in hot spring LCB003 using quality filtered reads from a previous sediment metagenome (IMG Genome ID 3300028675) (*24*).

Annotation and reconstruction of metabolic potential

MAGs were annotated with Prokka (version 1.14.6) and Interproscan (version 5.70-102.0) (*61*, *62*). Annotation refinement and confirmation was done by submission of protein sequences to the National Center for Biotechnology Information (NCBI) conserved domain database and HHpred using default settings. Sequences of [NiFe] hydrogenases (PF00374) were checked for conserved CXXC motifs at the N and C termini and submitted to HydDB for initial classification (*63*). Hydrogenase classification was further refined with phylogenetic analysis (below).

RNA extraction, sequencing, and analysis

Two replicate cultures were grown on 10 mM MMA under a N_2/CO_2 headspace. RNA was extracted from these cultures during active methane production. Culture bottles were cooled from 77°C by placing them in an ice bath that was then placed at −20°C for 15 min, and vials were subsequently kept on ice during the following procedure. Cells were rapidly concentrated onto sterivex filters, which were then cut open and placed into a Zymo BashingBead lysis tube (Zymo Research) containing 800 µl of TRIzol (Invitrogen) and vortexed at maximum speed for 20 min. The tubes were centrifuged at 14,000*g* for 15 min and the supernatant was used for RNA purification with the Zymo Direct-Zol kit according to the manufacturer's instructions and including the deoxyribonuclease (DNAse) I step. RNA extract from the replicate cultures was pooled, and purified RNA was used for library preparation and sequencing at SeqCenter (Pittsburgh, PA, USA). RNA was treated again with DNAse I (Invitrogen) and library preparation was performed with Illumina's Stranded Total RNA Prep Ligation with Ribo-Zero Plus kit and 10 bp unique dual indices. The library was sequenced on a NovaSeq X Plus platform, producing paired 2 × 150 bp reads. Demultiplexing, quality control, and adaptor trimming were performed with bcl-conver (version 4.1.5). Reads were further processed with rqcfilter2 (rna = t, trimrnaadapter = t, qtrim = rl, trimq = 10, maq = 20, maxns = 0, minlen = 50, mlf = 0.33, and removeribo = f) and mapped to reference genomes from the

YNP3N culture using salmon (version 1.10.2; --validateMappings --seqBias) (*64*). Reads mapping to rRNA genes were excluded before normalization. Reads mapping to each gene were normalized to gene length before calculating the center log ratio (log_{10}).

Phylogenetic analysis

A set of 43 single-copy marker proteins was collected from Nezhaarchaeia MAGs and reference archaeal genomes as previously described (*25*, *47*). Reference Nezhaarchaeia MAGs were collected from public databases and recent publications and only used if they were estimated at >75% completeness and had at least 37 of 43 phylogenomic marker proteins (*65*–*67*). These markers were aligned with MAFFT-linsi, trimmed with trimAL (-gt 0.7) and concatenated to produce a final alignment of 9913 positions (*68*, *69*). IQtree2 was used to reconstruct a maximum-likelihood phylogenetic tree using the best fit LG + F + R10 model and 1000 ultrafast bootstraps (*70*).

The YNP3N McrA protein sequence was extracted and aligned with reference archaeal McrA sequences with MAFFT-linsi, trimmed with trimAL (-gt 0.5), producing a final alignment of 556 positions. IQtree2 was used to reconstruct a maximum-likelihood phylogenetic tree using the LG + C60 + F + G model and 1000 ultrafast bootstraps.

Reference archaeal 16*S* rRNA sequences ≥1000 bp were aligned with the YNP3N 16S rRNA sequence using MAFFT-linsi and trimmed with trimAL (-automated1), producing an alignment of 1498 positions. IQtree2 was used to reconstruct a maximum-likelihood phylogenetic tree using the best-fit SYM + R8 model and 1000 ultrafast bootstraps.

Reference MtrA sequences were collected from diverse methanogenic and alkane degrading lineages and aligned with the YNP3N sequence using MAFFT-linsi and trimmed with trimAL (-automated1), producing an alignment of 242 positions. IQtree2 was used to reconstruct a maximum-likelihood phylogenetic tree using the best-fit LG + F + R6 model and 1000 ultrafast bootstraps.

Reference sequences of catalytic subunits of groups 1, 2, 3, and 4 [NiFe] hydrogenases (PF00374) and Fpo-like subunits (PF00346) were collected from HydDB and previous studies and aligned with sequences collected from Methanonezhaarchaeia genomes (*25*, *63*). Sequences were aligned using MAFFT-linsi and trimmed with trimAL (-gt 0.5), producing an alignment of 423 positions. IQtree2 was used to reconstruct a maximum-likelihood phylogenetic tree using the LG + C60 + F + G model and 1000 ultrafast bootstraps.

Fluorescence in situ hybridization

Subsamples of the YNP3N culture were fixed using 2% paraformaldehyde for 1 hour at room temperature as previously described (*25*). An oligonucleotide probe targeting most 16*S* rRNA sequences of Nezhaarchaea (equivalent to Terrestrial Miscellaneous Crenarchaeal Group in Silva release 138) was designed using the probe design tool in ARB (Mnez277, 5′-ACGGCCCGTACCCGTTATCG-3′). DOPE-FISH was performed as previously described (*25*) using the Mnez probe doubly labeled with Cy3 fluorophores (obtained from IDT-DNA) and a hybridization time of 3 hours at 10% formamide. Mnez277 was used in combination with the general archaeal probe Arch915, which was doubly labeled with Alexa Fluor 647 and cells were counterstained with the DNA stain 4′,6-diamidino-2-phenylindole (DAPI). Negative controls using double-labeled NON-EUB338 were performed in parallel.

Supplementary Materials

The PDF file includes:

Protolog
Figs. S1 to S5
Legends for tables S1 to S6

Other Supplementary Material for this manuscript includes the following:

Tables S1 to S6

REFERENCES AND NOTES

1. P. S. Garcia, S. Gribaldo, G. Borrel, Diversity and evolution of methane-related pathways in archaea. *Annu. Rev. Microbiol.* **76**, 727–755 (2022).
2. R. K. Thauer, A.-K. Kaster, H. Seedorf, W. Buckel, R. Hedderich, Methanogenic archaea: Ecologically relevant differences in energy conservation. *Nat. Rev. Microbiol.* **6**, 579–591 (2008).
3. P. S. Adam, G. E. Kolyfetis, T. L. Bornemann, C. E. Vorgias, A. J. Probst, Genomic remnants of ancestral methanogenesis and hydrogenotrophy in Archaea drive anaerobic carbon cycling. *Sci. Adv.* **8**, eabm9651 (2022).
4. Y. Wang, G. Wegener, T. A. Williams, R. Xie, J. Hou, C. Tian, Y. Zhang, F. Wang, X. Xiao, A methylotrophic origin of methanogenesis and early divergence of anaerobic multicarbon alkane metabolism. *Sci. Adv.* **7**, eabj1453 (2021).
5. Y. Ueno, K. Yamada, N. Yoshida, S. Maruyama, Y. Isozaki, Evidence from fluid inclusions for microbial methanogenesis in the early Archaean era. *Nature* **440**, 516–519 (2006).
6. J. M. Wolfe, G. P. Fournier, Horizontal gene transfer constrains the timing of methanogen evolution. *Nat. Ecol. Evol.* **2**, 897–903 (2018).
7. W. F. Martin, F. L. Sousa, Early microbial evolution: The age of anaerobes. *Cold Spring Harb. Perspect. Biol.* **8**, a018127 (2016).
8. M. Saunois, A. Martinez, B. Poulter, Z. Zhang, P. A. Raymond, P. Regnier, J. G. Canadell, R. B. Jackson, P. K. Patra, P. Bousquet, Global methane budget 2000–2020. *Earth System Sci. Data* **17**, 1873–1958 (2025).
9. D. Mayumi, H. Mochimaru, H. Tamaki, K. Yamamoto, H. Yoshioka, Y. Suzuki, Y. Kamagata, S. Sakata, Methane production from coal by a single methanogen. *Science* **354**, 222–225 (2016).
10. G. Borrel, P. S. Adam, L. J. McKay, L.-X. Chen, I. N. Sierra-García, C. M. Sieber, Q. Letourneur, A. Ghozlane, G. L. Andersen, W.-J. Li, Wide diversity of methane and short-chain alkane metabolisms in uncultured archaea. *Nat. Microbiol.* **4**, 603–613 (2019).
11. Z. Zhou, C.-j. Zhang, P.-f. Liu, L. Fu, R. Laso-Pérez, L. Yang, L.-p. Bai, J. Li, M. Yang, J.-z. Lin, Non-syntrophic methanogenic hydrocarbon degradation by an archaeal species. *Nature* **601**, 257–262 (2022).
12. L. J. McKay, M. Dlakić, M. W. Fields, T. O. Delmont, A. M. Eren, Z. J. Jay, K. B. Klingelsmith, D. B. Rusch, W. P. Inskeep, Co-occurring genomic capacity for anaerobic methane and dissimilatory sulfur metabolisms discovered in the Korarchaeota. *Nat. Microbiol.* **4**, 614–622 (2019).
13. I. Vanwonterghem, P. N. Evans, D. H. Parks, P. D. Jensen, B. J. Woodcroft, P. Hugenholtz, G. W. Tyson, Methylotrophic methanogenesis discovered in the archaeal phylum Verstraetearchaeota. *Nat. Microbiol.* **1**, 16170 (2016).
14. Y. Wang, G. Wegener, J. Hou, F. Wang, X. Xiao, Expanding anaerobic alkane metabolism in the domain of Archaea. *Nat. Microbiol.* **4**, 595–602 (2019).
15. Y.-F. Ou, H.-P. Dong, S. J. McIlroy, S. A. Crowe, S. J. Hallam, P. Han, J. Kallmeyer, R. L. Simister, A. Vuillemin, A. O. Leu, Expanding the phylogenetic distribution of cytochrome *b*-containing methanogenic archaea sheds light on the evolution of methanogenesis. *ISME J.* **16**, 2373–2387 (2022).
16. Z.-S. Hua, Y.-L. Wang, P. N. Evans, Y.-N. Qu, K. M. Goh, Y.-Z. Rao, Y.-L. Qi, Y.-X. Li, M.-J. Huang, J.-Y. Jiao, Insights into the ecological roles and evolution of methyl-coenzyme M reductase-containing hot spring Archaea. *Nat. Commun.* **10**, 4574 (2019).
17. K. Wu, L. Zhou, G. Tahon, L. Liu, J. Li, J. Zhang, F. Zheng, C. Deng, W. Han, L. Bai, Isolation of a methyl-reducing methanogen outside the Euryarchaeota. *Nature* **632**, 1124–1130 (2024).
18. J. Hou, Y. Wang, P. Zhu, N. Yang, L. Liang, T. Yu, M. Niu, K. Konhauser, B. J. Woodcroft, F. Wang, Taxonomic and carbon metabolic diversification of Bathyarchaeia during its coevolution history with early Earth surface environment. *Sci. Adv.* **9**, eadf5069 (2023).
19. P. N. Evans, D. H. Parks, G. L. Chadwick, S. J. Robbins, V. J. Orphan, S. D. Golding, G. W. Tyson, Methane metabolism in the archaeal phylum Bathyarchaeota revealed by genome-centric metagenomics. *Science* **350**, 434–438 (2015).
20. D. Y. Sorokin, K. S. Makarova, B. Abbas, M. Ferrer, P. N. Golyshin, E. A. Galinski, S. Ciordia, M. C. Mena, A. Y. Merkel, Y. I. Wolf, Discovery of extremely halophilic, methyl-reducing euryarchaea provides insights into the evolutionary origin of methanogenesis. *Nat. Microbiol.* **2**, 17081 (2017).
21. M. M. Lynes, Z. J. Jay, A. J. Kohtz, R. Hatzenpichler, Methylotrophic methanogenesis in the Archaeoglobi revealed by cultivation of Ca. Methanoglobus hypatiae from a Yellowstone hot spring. *ISME J.* **18**, wrae026 (2024).

22. S. Buessecker, G. L. Chadwick, M. E. Quan, B. P. Hedlund, J. A. Dodsworth, A. E. Dekas, Mcr-dependent methanogenesis in Archaeoglobaceae enriched from a terrestrial hot spring. *ISME J.* **17**, 1649–1659 (2023).
23. M. K. Nobu, T. Narihiro, K. Kuroda, R. Mei, W.-T. Liu, Chasing the elusive Euryarchaeota class WSA2: Genomes reveal a uniquely fastidious methyl-reducing methanogen. *ISME J.* **10**, 2478–2487 (2016).
24. V. Krukenberg, A. J. Kohtz, Z. J. Jay, R. Hatzenpichler, Methyl-reducing methanogenesis by a thermophilic culture of Korarchaeia. *Nature* **632**, 1131–1136 (2024).
25. A. J. Kohtz, N. Petrosian, V. Krukenberg, Z. J. Jay, M. Pilhofer, R. Hatzenpichler, Cultivation and visualization of a methanogen of the phylum Thermoproteota. *Nature* **632**, 1118–1123 (2024).
26. K. Pfeifer, İ. Ergal, M. Koller, M. Basen, B. Schuster, S. K.-M. Rittmann, Archaea biotechnology. *Biotechnol. Adv.* **47**, 107668 (2021).
27. C. P. Bueno de Mesquita, D. Wu, S. G. Tringe, Methyl-based methanogenesis: An ecological and genomic review. *Microbiol. Mol. Biol. Rev.* **87**, e00024-22 (2023).
28. N. Dombrowski, A. P. Teske, B. J. Baker, Expansive microbial metabolic versatility and biodiversity in dynamic Guaymas Basin hydrothermal sediments. *Nat. Commun.* **9**, 4999 (2018).
29. J. Wang, Y.-N. Qu, P. N. Evans, Q. Guo, F. Zhou, M. Nie, Q. Jin, Y. Zhang, X. Zhai, M. Zhou, Evidence for nontraditional mcr-containing archaea contributing to biological methanogenesis in geothermal springs. *Sci. Adv.* **9**, eadg6004 (2023).
30. M. M. Lynes, V. Krukenberg, Z. J. Jay, A. J. Kohtz, C. A. Gobrogge, R. L. Spietz, R. Hatzenpichler, Diversity and function of methyl-coenzyme M reductase-encoding archaea in Yellowstone hot springs revealed by metagenomics and mesocosm experiments. *ISME Commun.* **3**, 22 (2023).
31. K. Lang, J. Schuldes, A. Klingl, A. Poehlein, R. Daniel, A. Brune, New mode of energy metabolism in the seventh order of methanogens as revealed by comparative genome analysis of "Candidatus Methanoplasma termitum". *Appl. Environ. Microbiol.* **81**, 1338–1352 (2015).
32. A. Mahapatra, A. Patel, J. A. Soares, R. C. Larue, J. K. Zhang, W. W. Metcalf, J. A. Krzycki, Characterization of a Methanosarcina acetivorans mutant unable to translate UAG as pyrrolysine. *Mol. Microbiol.* **59**, 56–66 (2006).
33. G. Borrel, N. Parisot, H. M. Harris, E. Peyretaillade, N. Gaci, W. Tottey, O. Bardot, K. Raymann, S. Gribaldo, P. Peyret, Comparative genomics highlights the unique biology of Methanomassiliicoccales, a Thermoplasmatales-related seventh order of methanogenic archaea that encodes pyrrolysine. *BMC Genomics* **15**, 679 (2014).
34. B. Hao, W. Gong, T. K. Ferguson, C. M. James, J. A. Krzycki, M. K. Chan, A new UAG-encoded residue in the structure of a methanogen methyltransferase. *Science* **296**, 1462–1466 (2002).
35. F. Xie, S. Zhao, X. Zhan, Y. Zhou, Y. Li, W. Zhu, P. B. Pope, G. T. Attwood, W. Jin, S. Mao, Unraveling the phylogenomic diversity of Methanomassiliicoccales and implications for mitigating ruminant methane emissions. *Genome Biol.* **25**, 32 (2024).
36. O. M. Sokolovskaya, A. N. Shelton, M. E. Taga, Sharing vitamins: Cobamides unveil microbial interactions. *Science* **369**, eaba0165 (2020).
37. T. D. Mand, W. W. Metcalf, Energy conservation and hydrogenase function in methanogenic archaea, in particular the genus Methanosarcina. *Microbiol. Mol. Biol. Rev.* **83**, e00020-19 (2019).
38. J. Meuer, H. C. Kuettner, J. K. Zhang, R. Hedderich, W. W. Metcalf, Genetic analysis of the archaeon Methanosarcina barkeri Fusaro reveals a central role for Ech hydrogenase and ferredoxin in methanogenesis and carbon fixation. *Proc. Natl. Acad. Sci. U.S.A.* **99**, 5632–5637 (2002).
39. R. K. Thauer, The Wolfe cycle comes full circle. *Proc. Natl. Acad. Sci. U.S.A.* **109**, 15084–15085 (2012).
40. W. F. Fricke, H. Seedorf, A. Henne, M. Krüer, H. Liesegang, R. Hedderich, G. Gottschalk, R. K. Thauer, The genome sequence of Methanosphaera stadtmanae reveals why this human intestinal archaeon is restricted to methanol and H2 for methane formation and ATP synthesis. *J. Bacteriol.* **188**, 642–658 (2006).
41. G. Borrel, P. S. Adam, S. Gribaldo, Methanogenesis and the Wood–Ljungdahl pathway: An ancient, versatile, and fragile association. *Genome Biol. Evol.* **8**, 1706–1711 (2016).
42. T. Wagner, J. Koch, U. Ermler, S. Shima, Methanogenic heterodisulfide reductase (HdrABC-MvhAGD) uses two noncubane [4Fe-4S] clusters for reduction. *Science* **357**, 699–703 (2017).
43. K. C. Costa, P. M. Wong, T. Wang, T. J. Lie, J. A. Dodsworth, I. Swanson, J. A. Burn, M. Hackett, J. A. Leigh, Protein complexing in a methanogen suggests electron bifurcation and electron delivery from formate to heterodisulfide reductase. *Proc. Natl. Acad. Sci. U.S.A.* **107**, 11050–11055 (2010).
44. T. Wagner, U. Ermler, S. Shima, The methanogenic CO_2 reducing-and-fixing enzyme is bifunctional and contains 46 [4Fe-4S] clusters. *Science* **354**, 114–117 (2016).
45. O. N. Lemaire, T. Wagner, All-in-One CO_2 capture and transformation: Lessons from formylmethanofuran dehydrogenases. *Acc. Chem. Res.* **57**, 3512–3523 (2024).
46. T. Watanabe, O. Pfeil-Gardiner, J. Kahnt, J. Koch, S. Shima, B. J. Murphy, Three-megadalton complex of methanogenic electron-bifurcating and CO_2-fixing enzymes. *Science* **373**, 1151–1156 (2021).
47. A. J. Kohtz, Z. J. Jay, M. M. Lynes, V. Krukenberg, R. Hatzenpichler, Culexarchaeia, a novel archaeal class of anaerobic generalists inhabiting geothermal environments. *ISME Commun.* **2**, 86 (2022).
48. M. F. Abdul Halim, L. A. Day, K. C. Costa, Formate-dependent heterodisulfide reduction in a *Methanomicrobiales* archaeon. *Appl. Environ. Microbiol.* **87**, e02698-20 (2021).
49. K. C. Costa, S. H. Yoon, M. Pan, J. A. Burn, N. S. Baliga, J. A. Leigh, Effects of H_2 and formate on growth yield and regulation of methanogenesis in *Methanococcus maripaludis*. *J. Bacteriol.* **195**, 1456–1462 (2013).
50. P. Liu, Y. Lu, Concerted metabolic shifts give new insights into the syntrophic mechanism between propionate-fermenting *Pelotomaculum thermopropionicum* and hydrogenotrophic *Methanocella conradii*. *Front. Microbiol.* **9**, 1551 (2018).
51. I. Aziz, K. Kayastha, S. Kaltwasser, J. Vonck, S. Welsch, B. J. Murphy, J. Kahnt, D. Wu, T. Wagner, S. Shima, Structural and mechanistic basis of the central energy-converting methyltransferase complex of methanogenesis. *Proc. Natl. Acad. Sci. U.S.A.* **121**, e2315568121 (2024).
52. Y.-L. Qi, P. N. Evans, Y.-X. Li, Y.-Z. Rao, Y.-N. Qu, S. Tan, J.-Y. Jiao, Y.-T. Chen, B. P. Hedlund, W.-S. Shu, Comparative genomics reveals thermal adaptation and a high metabolic diversity in "*Candidatus* Bathyarchaeia". *Msystems* **6**, e0025221 (2021).
53. M. Kolmogorov, D. M. Bickhart, B. Behsaz, A. Gurevich, M. Rayko, S. B. Shin, K. Kuhn, J. Yuan, E. Polevikov, T. P. Smith, metaFlye: Scalable long-read metagenome assembly using repeat graphs. *Nat. Methods* **17**, 1103–1110 (2020).
54. G. Bouras, L. M. Judd, R. A. Edwards, S. Vreugde, T. P. Stinear, R. R. Wick, How low can you go? Short-read polishing of Oxford Nanopore bacterial genome assemblies. *Microb. Genom.* **10**, 001254 (2024).
55. R. R. Wick, K. E. Holt, Polypolish: Short-read polishing of long-read bacterial genome assemblies. *PLoS Comput. Biol.* **18**, e1009802 (2022).
56. D. Li, C.-M. Liu, R. Luo, K. Sadakane, T.-W. Lam, MEGAHIT: An ultra-fast single-node solution for large and complex metagenomics assembly via succinct de Bruijn graph. *Bioinformatics* **31**, 1674–1676 (2015).
57. H. Li, Minimap2: Pairwise alignment for nucleotide sequences. *Bioinformatics* **34**, 3094–3100 (2018).
58. D. H. Parks, M. Imelfort, C. T. Skennerton, P. Hugenholtz, G. W. Tyson, CheckM: Assessing the quality of microbial genomes recovered from isolates, single cells, and metagenomes. *Genome Res.* **25**, 1043–1055 (2015).
59. P.-A. Chaumeil, A. J. Mussig, P. Hugenholtz, D. H. Parks, GTDB-Tk v2: Memory friendly classification with the genome taxonomy database. *Bioinformatics* **38**, 5315–5316 (2022).
60. S. T. Aroney, R. J. Newell, J. N. Nissen, A. P. Camargo, G. W. Tyson, B. J. Woodcroft, CoverM: Read alignment statistics for metagenomics. *Bioinformatics* **41**, btaf147 (2025).
61. T. Seemann, Prokka: Rapid prokaryotic genome annotation. *Bioinformatics* **30**, 2068–2069 (2014).
62. P. Jones, D. Binns, H.-Y. Chang, M. Fraser, W. Li, C. McAnulla, H. McWilliam, J. Maslen, A. Mitchell, G. Nuka, InterProScan 5: Genome-scale protein function classification. *Bioinformatics* **30**, 1236–1240 (2014).
63. D. Søndergaard, C. N. Pedersen, C. Greening, HydDB: A web tool for hydrogenase classification and analysis. *Sci. Rep.* **6**, 34212 (2016).
64. R. Patro, G. Duggal, M. I. Love, R. A. Irizarry, C. Kingsford, Salmon provides fast and bias-aware quantification of transcript expression. *Nat. Methods* **14**, 417–419 (2017).
65. T. S. Schmidt, A. Fullam, P. Ferretti, A. Orakov, O. M. Maistrenko, H.-J. Ruscheweyh, I. Letunic, Y. Duan, T. Van Rossum, S. Sunagawa, SPIRE: A Searchable, Planetary-scale mIcrobiome REsource. *Nucleic Acids Res.* **52**, D777–D783 (2024).
66. S. Nayfach, S. Roux, R. Seshadri, D. Udwary, N. Varghese, F. Schulz, D. Wu, D. Paez-Espino, I.-M. Chen, M. Huntemann, A genomic catalog of Earth's microbiomes. *Nat. Biotechnol.* **39**, 499–509 (2021).
67. Y.-L. Qi, Y.-T. Chen, Y.-G. Xie, Y.-X. Li, Y.-Z. Rao, M.-M. Li, Q.-J. Xie, X.-R. Cao, L. Chen, Y.-N. Qu, Analysis of nearly 3000 archaeal genomes from terrestrial geothermal springs sheds light on interconnected biogeochemical processes. *Nat. Commun.* **15**, 4066 (2024).
68. K. Katoh, D. M. Standley, MAFFT multiple sequence alignment software version 7: Improvements in performance and usability. *Mol. Biol. Evol.* **30**, 772–780 (2013).
69. S. Capella-Gutiérrez, J. M. Silla-Martínez, T. Gabaldón, trimAl: A tool for automated alignment trimming in large-scale phylogenetic analyses. *Bioinformatics* **25**, 1972–1973 (2009).
70. B. Q. Minh, H. A. Schmidt, O. Chernomor, D. Schrempf, M. D. Woodhams, A. Von Haeseler, R. Lanfear, IQ-TREE 2: New models and efficient methods for phylogenetic inference in the genomic era. *Mol. Biol. Evol.* **37**, 1530–1534 (2020).

Acknowledgments: We thank the US National Park Service for permitting work in Yellowstone National Park under permit number YELL-SCI-8010. We thank the Shell Research and Innovation–Nature-Based Solutions (NBS) Program for providing access to the LI-COR instrumentation used for gas flux data collection in this study, and S. Joye and R. Sibert (both University of Georgia) for conducting hot spring methane flux measurements. We thank N. Matos-Vega and W. Christian (both Montana State University) for assistance with H_2 and ^{13}C-GCMS measurements, and Z.J. Jay (Montana State University) for helpful discussions. **Funding:** This

work was supported by the U.S. Department of Energy, Office of Science, Biological and Environmental Research DE-SC0025661 (R.H.) and U.S. National Science Foundation, Biological Oceanography OCE-2049445 (R.H.). **Author contributions:** Conceptualization: A.J.K. and R.H. Methodology: A.J.K. and S.N. Validation: A.J.K. and R.H. Formal analysis: A.J.K. Investigation: A.J.K. and S.N. Resources: R.H. Data curation: A.J.K. and S.N. Writing–original draft: A.J.K. Writing–review and editing: A.J.K., S.N., and R.H. Visualization: A.J.K. Supervision: R.H. Project administration: A.J.K. and R.H. Funding acquisition: R.H. **Competing interests:** The authors declare that they have no competing interests. **Data and materials availability:** Metagenomic and metatranscriptomic data were deposited on NCBI under the Project ID PRJNA1272160, https://www.ncbi.nlm.nih.gov/bioproject/PRJNA1272160/. The assembled YNP3N genome and associated culture MAGs were deposited on Zenodo (https://doi.org/10.5281/zenodo.17576686). All data needed to evaluate the conclusions in the paper are present in the paper and/or the Supplementary Materials.

Submitted 25 June 2025
Accepted 12 November 2025
Published 12 December 2025
10.1126/sciadv.aea0936

Science Advances
AAAS

Supplementary Materials for

Cultivation of Methanonezhaarchaeia, the third class of methanogens within the phylum Thermoproteota

Anthony J. Kohtz *et al.*

Corresponding author: Anthony J. Kohtz, anthony.kohtz@monash.edu;
Roland Hatzenpichler, rolandhatzenpichler@gmail.com

Sci. Adv. **11**, eaea0936 (2025)
DOI: 10.1126/sciadv.aea0936

The PDF file includes:

Protolog
Figs. S1 to S5
Legends for tables S1 to S6

Other Supplementary Material for this manuscript includes the following:

Tables S1 to S6

Protologue

Class
Candidatus Methanonezhaarchaeia class nov.
Me.tha.no.ne.zha.ar.chae'ia. N.L. neut. n. Methanonezhaarchaeales, type order of the class. L. -ia, ending to designate a class; N.L. fem. pl. n. Methanonezhaarchaeia, the Methanonezhaarchaeum class. The description is the same as for Methanonezhaarchaeum gen. nov.

Order
Candidatus Methanonezhaarchaeales order nov.
Me.tha.no.ne.zha.ar.chae'ales. N.L. neut. n. Methanonezhaarchaeceae, type family of the order. L. -ales, ending to designate an order; Methanonezhaarchaeales, the Methanonezhaarchaeum order. The description is the same as for Methanonezhaarchaeum gen. nov.

Family
Candidatus Methanonezhaarchaeceae fam. nov.
Me.tha.no.ne.zha.ar.chae'ceae. N.L. neut. n. Methanonezhaarchaeum, type genus of the family. L. -ceae, ending to designate a family; Methanonezhaarchaeaceae, the Methanonezhaarchaeum family. The description is the same as for Methanonezhaarchaeum gen. nov.

Genus
Candidatus Methanonezhaarchaeum gen. nov.
Me.tha.no.ne.zha.ar.chae'eum. N.L. pref. methano- pertaining to methane metabolism; N.L. neut. n. archaeum, "ancient", identifying this cell as a member of the domain Archaea; N.L. neut. n. Methanonezhaarchaeum, methanogenic archaeon named after Nezha, an immortal in Chinese mythology[14]. The type species is *Candidatus* Methanonezhaarchaeum fastidiosum sp. nov.

Species
Candidatus Methanonezhaarchaeum fastidiosum sp. nov.
fas.ti.di.o'sum L. neut, adj. fastidiosum, referring to the fastidious growth of this organism. This archaeon was cultured from an unnamed hot spring in Yellowstone National Park that we identified as feature LCB003 in a recent survey[30]. The organism is an obligate anaerobic thermophile that performs methyl-dismutating methanogenesis and grows as coccoid cells.

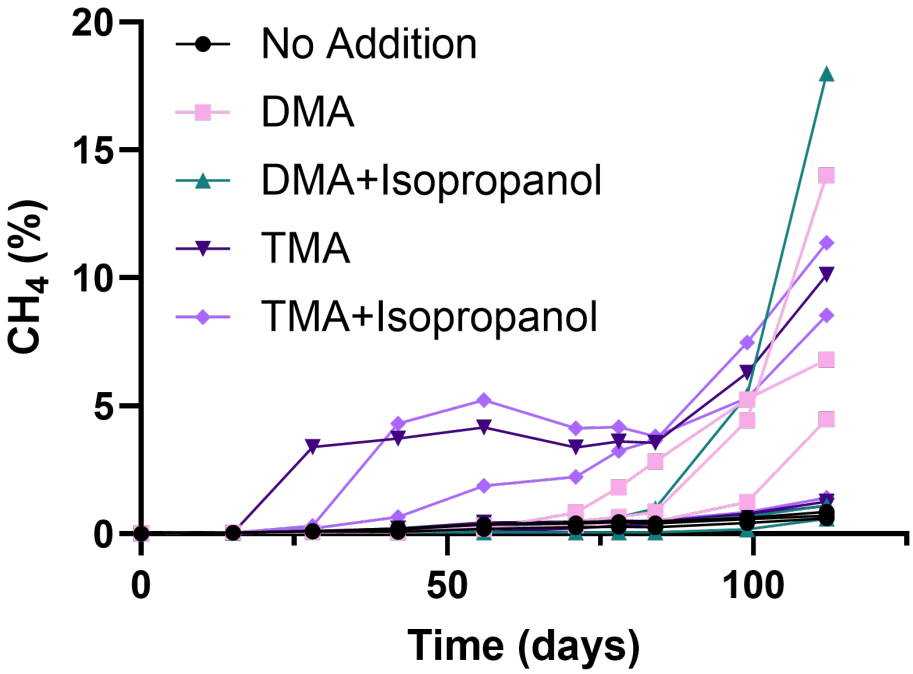

Fig. S1. Methane production in incubations with dimethylamine (DMA) and trimethylamine (TMA), with or without isopropanol. Each individual biological replicate is shown (n=3 for each condition). Methylamines and isopropanol were added at 10 mM final concentration.

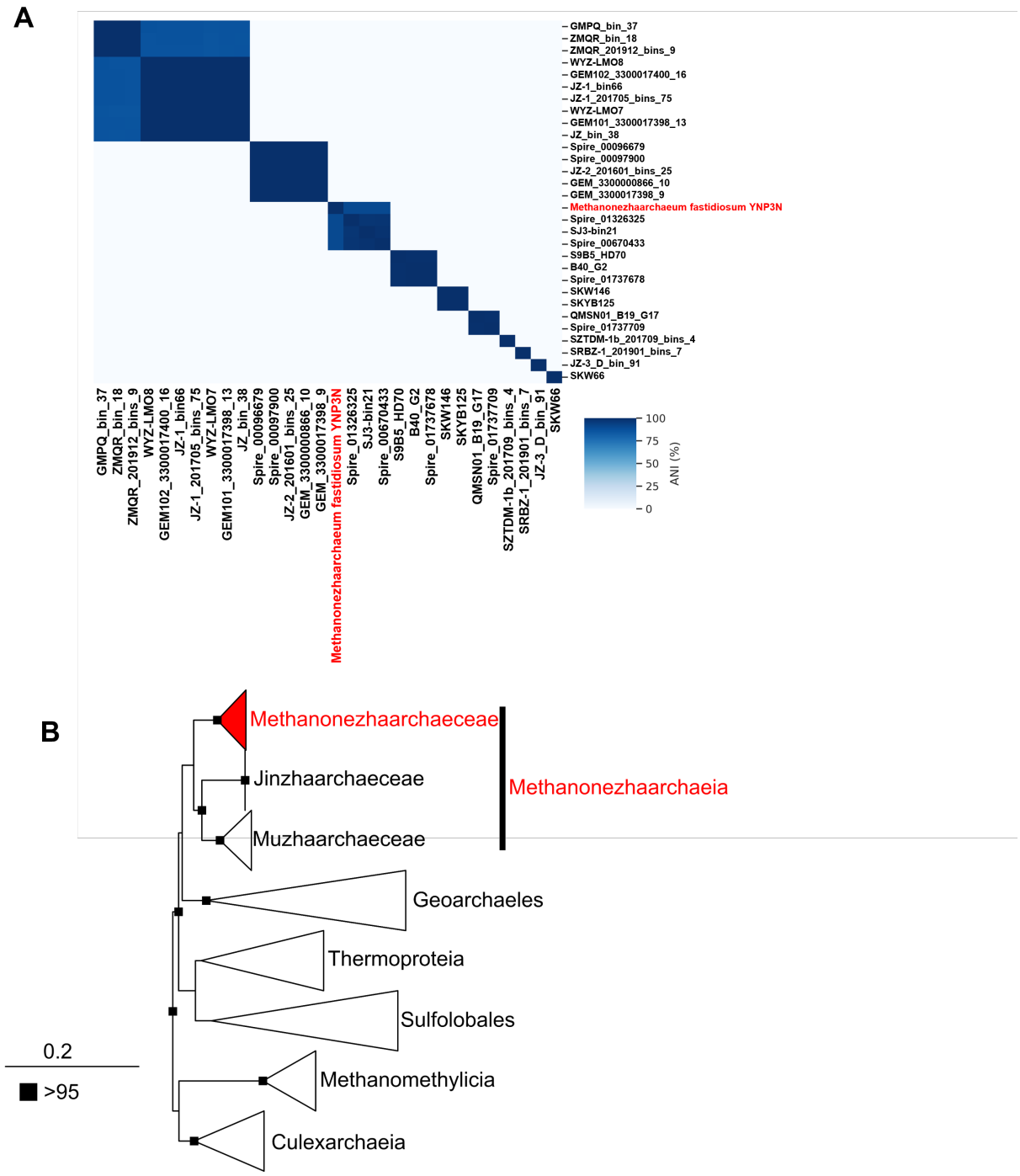

Fig. S2. Average Nucleotide Identity (ANI) and phylogenetic analysis of 16S rRNA. (A) ANI clusters across the Methanonezhaarchaeia showing placement of YNP3N as a separate species cluster. **(B)** Phylogenetic tree of the 16S rRNA showing YNP3N clustering within the Methanonezhaarchaeia. Squares at the nodes indicate ultrafast bootstrap support, only values above 95 are shown.

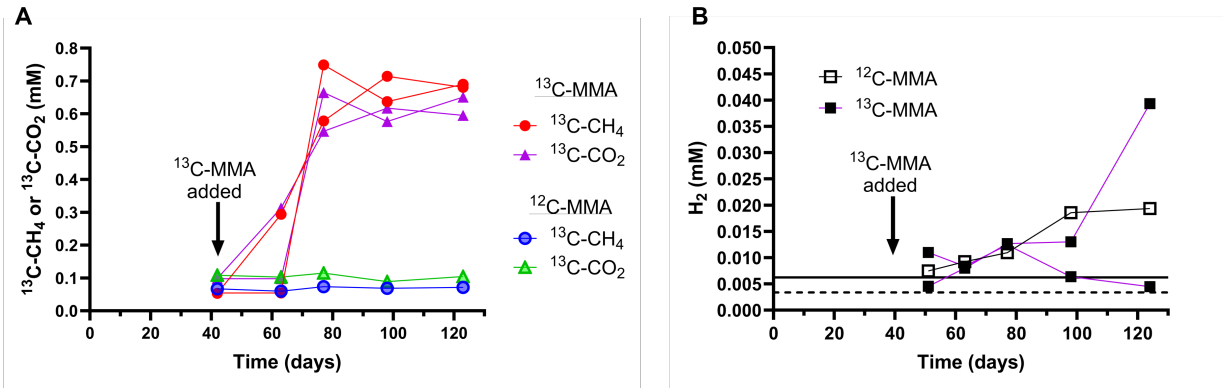

Fig. S3. Incubations of M. fastidiosum YNP3N with ^{13}C-MMA and H_2 measurements. (A) ^{13}C-CH_4 and ^{13}C-CO_2 production in cultures amended with ^{13}C-MMA or ^{12}C-MMA. Incubations were initiatedwith 10 mM ^{12}C-MMA, and on day 42 were spiked with an additional 2 mM of either ^{12}C- or ^{13}C-MMA. ^{13}C-CH_4 and ^{13}C-CO_2 are produced when incubated with ^{13}C-MMA, consistent with methyl-dismutation. **(B)** H_2 concentrations in bottles amended with ^{13}C-MMA and ^{12}C-MMA. Background signals of gas tanks used for anoxic conditions are shown (N_2 gas, solid line; N_2:CO_2 (90:10) tank, dashed line). The absence of H_2 accumulation is consistent with the methyl-dismutating and hydrogen cycling model of strain YNP3N's metabolism.

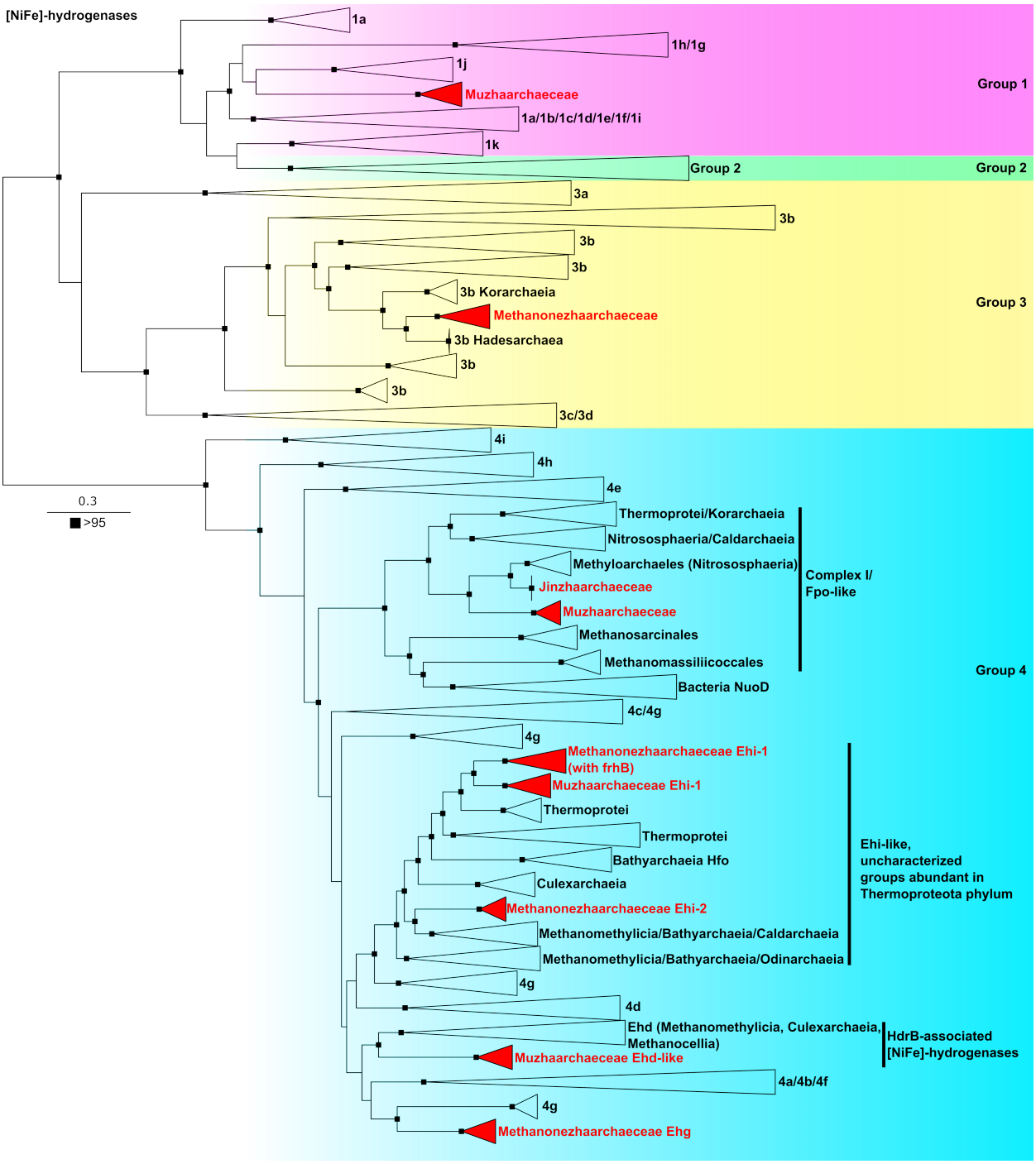

Fig. S4. Phylogenetic tree of group 1, 2, 3, and 4 [NiFe] hydrogenases found in Methanonezhaarchaeia genomes (red). The phylogenetic tree was constructed from an alignment of 423 positions and the LG+C60+F+G model. Squares at the nodes indicate ultrafast bootstrap support, only values above 95 are shown.

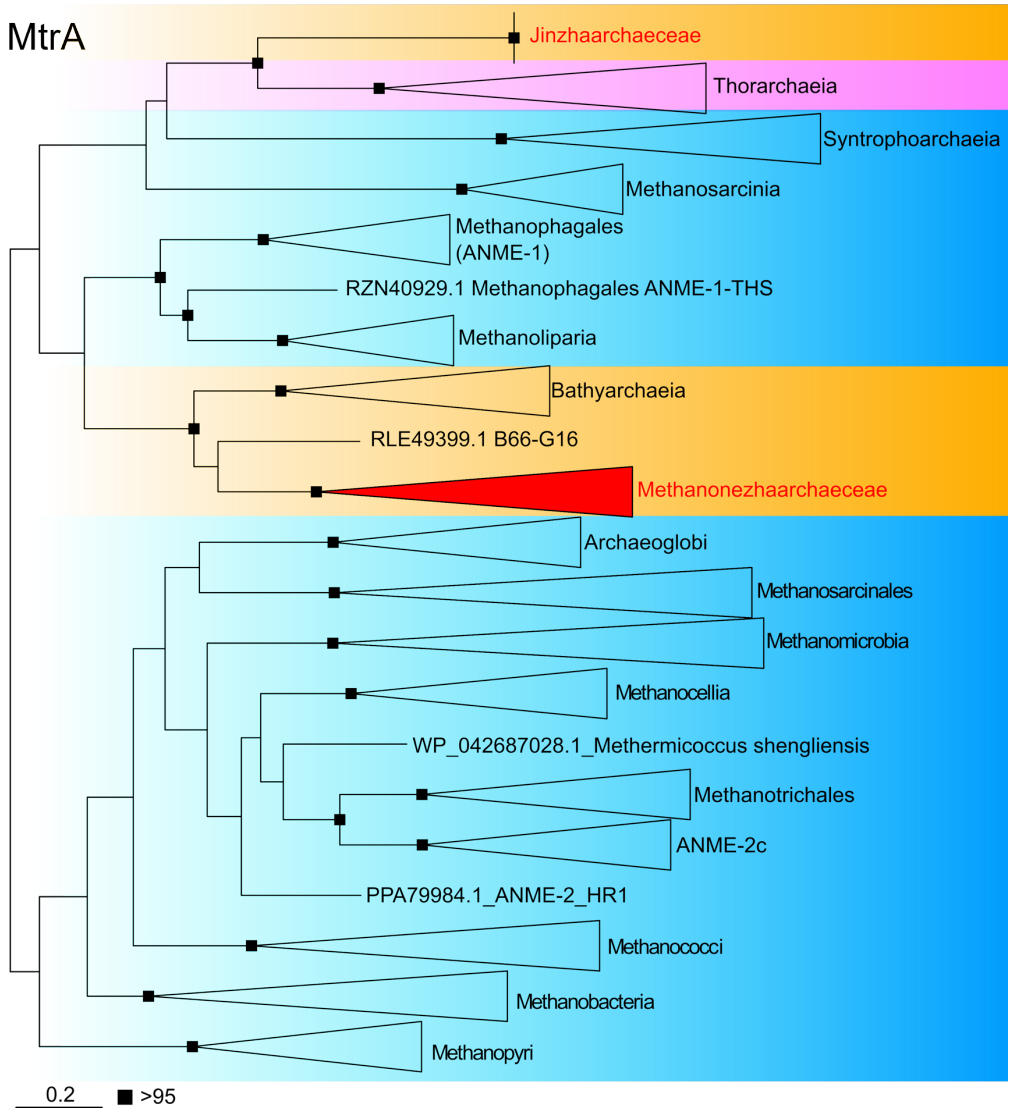

Fig. S5. Phylogenetic tree of MtrA sequences collected from reference archaeal genomes and Methanonezhaarchaeia. Two separate lineages are found in Methanonezhaarchaecea and Jinzhaarchaecea (red). The phylogenetic tree was constructed from an alignment of 242 positions, the best fit LG+F+R6 model, and 1,000 ultrafast bootstraps.

Table S1 (separate sheet in xls file)
Summary of the Ca. M. fastidiosum YNP3N genome, and other Metagenome Assembled Genomes (MAGs) recovered from the enrichment metagenome.

Table S2 (separate sheet in xls file)
Distribution of 16S rRNA genes affiliated with Methanonezhaarchaeum in NCBI and IMG databases.

Table S3 (separate sheet in xls file)
Distribution of mcrA genes affiliated with Methanonezhaarchaeum in IMG databases.

Table S4 (separate sheet in xls file)
Summary of metatranscriptomic data shown in Figure 3B.

Table S5 (separate sheet in xls file)
Reference genomes of Methanonezhaarchaeia.

Table S6 (separate sheet in xls file)
Presence and absence of methanogenesis marker proteins in Methanonezhaarchaeia MAGs.